ARTICLE

https://doi.org/10.1590/2317-4889202120200073

BJGEO
Brazilian Journal of Geology

Geochemical evolution of soils developed from pyroclastic rocks of Trindade Island, South Atlantic

Ana Carolina Campos Mateus[1]*, Angélica Fortes Drummond Chicarino Varajão[1], Fábio Soares de Oliveira[2], Sabine Petit[3], Carlos Ernesto Gonçalves Reynaud Schaefer[4]

Abstract

The geochemical behavior of the major, minor, trace and rare earths elements (REEs) in soil profiles from ultramafic volcanoclastic rocks of the Vulcão do Paredão and Morro Vermelho Formation from Trindade Island (TI) was analyzed in this study. Losses and gains of chemical elements were calculated through the mass balance for two profiles along the slope: one located at higher altitude (460 m) and the other at lower altitude (258 m). In all profiles, Al, Fe and Ti accumulate due to their low mobility, whereas Ca, Na, K and Mg are the most intensely leached. Soils located at lower altitude show higher K and Mg values in the surface due to the contribution of saline sprays. Leaching of the REEs from higher to the lower slope led to the enrichment of these elements, especially the light REEs, in the soil at the lowest altitude (258 m). The high altitude profile showed Ce positive anomaly due to longer exposure to weathering. The geochemical balance shows a relative enrichment of Ti, Mn, Fe, Co, Cr, Ni, V, Zr, S related to the loss of mobile elements during the soil formation process, despite the youthful nature of these volcanic rocks.

KEYWORDS: Geochemical balance, REEs, Inductively coupled plasma atomic emission spectroscopy (ICP-AES).

INTRODUCTION

The distribution and migration of the chemical elements, and the chemical reactions during weathering and soil formation processes are essential in pedogeochemical studies (Carvalho 1995). The meteoric water reacts with most rock minerals, and new stable mineral phases are formed under new physicochemical conditions (Carvalho 1995, Putnis 2009). In this process, some chemical elements are leached out, while others are concentrated.

The chemical reactions occurring during the soil formation determine the mobilization and redistribution of elements within the soil profile, and a significant correlation can be recorded between the total concentration of elements in soils and parent material (Roca *et al.* 2008). To study the distribution and migration of chemical elements along the soil profile, the chemical mass balance between the parent material and the alteration products is used, an isovolumetric change (Millot and Bonifas 1955, Gardner 1980, Cramer and Nesbitt 1983).

In the Brazilian territory, there are few studies on the geochemistry of soils from volcanic oceanic islands, specifically on the latest pyroclasts. Of the existing studies, few report the geochemical evolution of soil formation. Among them, there are the studies of Oliveira *et al.* (2014) that showed the soil phosphatization process of Rata Island (Fernando de Noronha Archipelago) due to the interaction of bird excrement with olivine nephelinites (ankaratritic lavas), and of Oliveira *et al.* (2009) that report high contents of Cu, Pb, Zn, As, U, and Sr in besides soils of this island due to the interaction of guano with mafic rocks, and anomalous concentrations of Ba, Nb, Ta, Cr, Hf, V and Zr due to the geochemical inheritance of local basalts. In the Fernando de Noronha Island, Oliveira *et al.* (2011b) showed that soils developed from mafic rocks (nepheline basalts) presented higher contents of Fe, Co, Ni and Cr, and Oliveira *et al.* (2011a) showed that soils from these rocks concentrate rare earth elements (REEs), preferably the heavy REEs (HREEs).

In reddened topsoil developed on mafic lapilli from Fogo island (Cape Verde), the upper level shows a significant gain of Na, Cr, P, Si, and particularly As, and the hematite may explain the significant retention of Cr, P, As and light REEs (LREE) in the topsoil (Marques *et al.* 2014).

In soils of basaltic rocks of Cameroon, the organic matter may account for low mobility of Cu and Pb, and the Mn-Al system may control Zn retardation at low elevations (Manga *et al.* 2016).

In basaltic pyroclasts from Azores, there are studies on the behavior of REEs (Freitas and Pacheco 2010, Vieira *et al.*

[1]Geology Department, Universidade Federal de Ouro Preto – Ouro Preto (MG), Brazil. E-mails: anacamposeg@hotmail.com, angelica@degeo.ufop.br

[2]Geoscinces Institute, Geography Department, Universidade Federal de Minas Gerais – Belo Horizonte (MG), Brazil. E-mail: fabiosolos@gmail.com

[3]Institut de Chimie des Mileux et Materiaux de Poitiers, Université de Poitiers – Poitiers, France. E-mail: sabine.petit@univ-poitiers.fr

[4]Soil Science Department, Universidade Federal de Viçosa – Viçosa (MG), Brazil. E-mail: carlos.schaefer@ufv.br

*Corresponding author.

2004), showing a predominance in LREEs and positive Ce and Er negative anomalies. In soils developed on phonolitic pyroclasts in Cape Verde also occur positive Ce anomalies (Marques *et al.* 2018).

In Trindade Island, despite studies by Clemente *et al.* (2012) have shown the availability of trace elements in soils from different eruptive materials, there are deficiencies in studies showing the behavior of chemical elements in these soils, including REEs and the chemical mass balance. To fill this gap, the present study aims to bring more information about the geochemical evolution from the pyroclasts to the soil and to evaluate the distribution and quantification of losses and gains of major, minor, trace and REEs.

METHODOLOGY

The sampling was carried out along four alteration profiles covering the pedological horizons and semi-altered ultramafic pyroclastic rocks of the Vulcão do Paredão and Morro Vermelho Formation, located at different altitudes of Trindade Island (Fig. 1). The Trindade island has a tropical oceanic climate with average annual rainfall between 926 mm and a marked dry season between January and March. The annual mean temperature is 25°C, being March the warmest month of the year and June the coolest (Fund 2014).

The undeformed soil samples were collected by using a volumetric ring, maintaining the original structure of the material to determine the apparent density.

Chemical analyzes

For the chemical analyzes, the samples of weathered rocks and soils were air-dried and then manually sprayed in agate mortar and sieved to 150# (granulometry less than 0.105 mm), individualizing aliquots of about 50 g.

The chemical analyzes of the major (Al, Fe, K, Mg, Na, Ca, P), minor (Ti, Mn) and trace elements (Ba, Co, Cr, Cu, Li, Ni, Sr, Th, V, Zn, Be, Zr, S, Sc, Ga, Y, Cd, In, Cs, Tl, Pb, Bi, U) were obtained by inductively coupled plasma optical emission spectrometry (ICP-OES) Agilent Technologies 725 while the REEs by inductively coupled plasma mass spectrometry (ICP-MS) Agilent Technologies 7700 at the LGqa Laboratory of Geology Department at Universidade Federal de Ouro Preto (DEGEO/UFOP). For total digestion of 0.1g of each sample, 1 mL of hydrogen peroxide as added for the removal of organic matter. After total removal of organic matter, they were added 3 mL of HCl per 10 mol L^{-1} and 6 mL of HNO_3 per 10 mol L^{-1}, 20 mL of HNO_3 per 2 mol L^{-1} for digestion of carbonates and oxides and 4 mL of HF concentrate for digestion of silicates. The percentage of SiO_2 was calculated in a relative way by the difference to 100% in the sum of the main elements and loss on ignition (LOI). The standard used as reference to rocks was the basalt certified (Cotta *et al.* 2008).

Apparent bulk density, absolute contents and geochemical balance

For this analysis, the most complete profiles 1 and 3 were chosen, including, at the base, the presence of pyroclasts and, at the top, the A horizon.

The determination of bulk density was made for the weathered rocks by paraffin clod method and for the soils by volumetric ring method (Teixeira *et al.* 2017).

The density values were incorporated in the calculation of losses and gains of the elements from the altered rock to the soil, so that the volume variation could be fixed. The absolute contents of each chemical component of profiles 1 and 3 were then calculated using the contents of the elements obtained by chemical analysis and the density measurement of the respective samples. For the quantitative evaluation of the losses and gains of chemical elements during the pedogenetic processes, the chemical mass balance calculations were performed using the Millot and Bonifas (1955) precepts. The Equation 1 was used:

$$\{ [(Ea * Da) - (Epy * Dpy)] / (Epy * Dpy) \} * 100 \qquad (1)$$

In which:
Ea = the concentration of the element in horizon "a";
Da = the bulk density of horizon "a";
Epy = the concentration of the element in pyroclasts ;
Dpy = the bulk density of pyroclast.

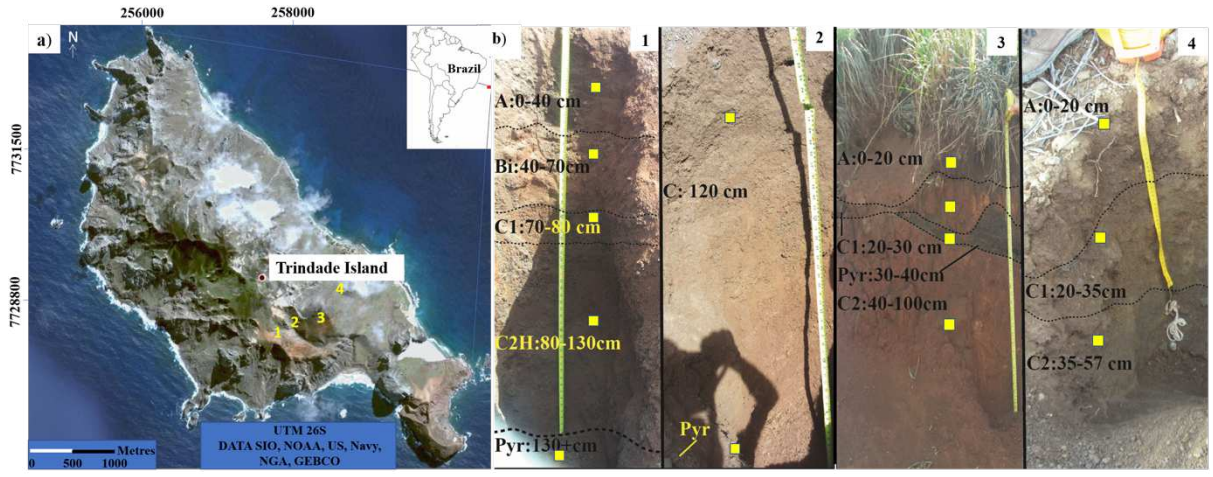

Source: modified of Mateus *et al.* (2018).

Figure 1. (A) Satellite image of Trindade Island with location of 1, 2, 3 and 4 profiles. (B) Image of profiles 1, 2, 3 and 4 showing sampling point.

Physical characteristics and mineralogy

Table 1 summarizes the main physical and mineralogical characteristics of the four soil profiles according Mateus *et al.* (2020a) and Mateus *et al.* (2018).

RESULTS

Geochemistry

Pyroclasts show the predominance of SiO_2, FeO_t, Al_2O_3, TiO_2, CaO, MgO and P_2O_5 among the major and minor elements (Tab. 2), due to the presence of forsterite, clinopyroxenes (augite and diopiside), Ti-biotite, Ti-magnetite, ilmenite and sideromelane (Tab. 1). In particular, CaO value in the profile 2 is high due to the presence of calcium zeolites (Ca-chabazite and Ca-heulandite) added to the presence of clinopyroxenes. K_2O, Na_2O and MnO occur in small quantities and are mainly related to volcanic glass (sideromelane), which constitutes approximately 50% of the rock. The quantification of volcanic glass was obtained by description of rocks previously impregnated in a Zeiss microscope fitted with a digital camera (Mateus *et al.* 2020a, 2020b). The pyroclasts from profile 3 contain K_2O values greater than Na_2O due to the higher amounts of Ti-biotite. The high LOI values are due to the presence of sideromelane and palagonite that contain water in their composition. Among the trace and REEs, Ba, Cr, Sr, V, Zr and Ce are those that show similar contents in all pyroclasts.

In all soil horizons occur the predominance of SiO_2, Al_2O_3, FeO_t, TiO_2 (Tab. 2). The high amounts of FeOt is mainly attributed the presence of semi-altered primary mineral such as Ti-magnetites and secondary minerals such as hematite, goethite and ferrihydrites (Tab. 1). TiO_2 is the fourth most abundant element in the profiles 1, 2 and 3, and its presence is related to the presence of rutile, anatase, biotite, magnetite and ilmenite.

The normalization of the REEs' concentrations to chondrite data show higher concentrations of LREEs in all profiles. The profile 1 have positive anomalies of Ce higher than other profiles (2, 3 and 4) (Tab. 3, Fig. 2).

Absolute contents and geochemical balance from profiles 1 and 3

Distribution diagrams (Figs. 3 and 4) were obtained by the relation of the absolute contents (Tab. 4) with the density values. This relationship with the geochemical balance results (Tab. 5) allows us to make the following inferences.

Profile 1

Among the major and minor elements, Si, Al, Fe and Ti show similar behavior. There is a pronounced decrease in absolute contents towards C2 horizon followed by a relative increase to the top of profile. Gains are higher in the Bi horizon with 66.83% Fe and 36.36% Ti, and in the C1 horizon with 40.25% Mn. Na, K, Ca, Mg and P also show similar comportment with a pronounced decrease to the top of the profile, but no peaks of increase. For Mg there is an increase peak in the C1 horizon with stabilization in the A and Bi horizons. Losses are higher in Ca and Na with values around 90% compared to the altered pyroclast.

Among the trace elements, the absolute contents of Ba, Co, Cr and Ni increase significantly towards the top, with moderate gain in the A horizon, reaching 87.55, 19.57, 125.57 and 79.16%, respectively, in the Bi horizon. For Cu, Th, V, Zn, Zr, S, Pb, Ca, Ga and U, there is a decrease from the rock to C2

Table 1. Physical and mineralogical characteristics of the profiles (Mateus *et al.* 2020a, 2020b) and Mateus *et al.* (2018).

Profile	Location and toposequence region	Altitude (m)	Source material and geological formation	Erosion degree	Mineralogy of pyroclastic rocks	Soil mineralogy
1	257867/7729600 top	460	Alic Hapludand pyroclast derivative Vulcão do Paredão	Extremely strong	Ol, Px, Bt, Mag, Ilm, Hem, sideromelane, sideromelane palagonitized	Ol, Px, Bt, Mag, Ilm, Hem, Hal, Fh, Gth, Ant, sideromelane palagonitized
2	257916/7729828 Upper middle strand	351	Typic Hapludand pyroclast derivative Morro Vermelho Formation	Extremely strong	Ol, Px, Bt, Mag, Ilm, Hem, Zl, sideromelane, sideromelane palagonitized	Ol, Px, Bt, Mag, Ilm, Hem, Hal, Fh, Gth, Rt, sideromelane palagonitized
3	258467/7729761 Lower middle strand	258	Typic Hapludand pyroclast derivative Morro Vermelho Formation	Extremely strong	Ol, Px, Bt, Mag, Ilm, Hem, sideromelane, sideromelane palagonitized	Ol, Px, Bt, Mag, Ilm, Hem, Hal, Fh, Gth, Rt, sideromelane palagonitized
4	258826/7730121 Strand of the coast; base	72	Typic Udipsamments pyroclast derivative Morro Vermelho Formation	Extremely strong	-	Ol, Px, Bt, Fd, Mag, Ilm, Hem, Hal, Fh, Gth, Rt

Bt: Ti-biotite; Ol: olivine (forsterite); Ilm: ilmenite; Px: pyroxenes (augite, diopside); Mag: magnetite; Fp: feldspars (anorthoclase, oligoclase); Zl: zeolite (chabazite, heulandite); Hem: hematite; Gth: goethite; Ant: anatase; Rt: rutile; Hall: halloysite; Fh: Ferryhidrite.

Table 2. Bulk chemistry contents of major, minor, trace elements, and rare earths elements from the soil profiles 1, 2, 3 and 4.

	1					2		3				4		
	A	**Bi**	**C1**	**C2**	**Py**	**C**	**Py**	**A**	**C1**	**C2**	**Py**	**A**	**C1**	**C2**
							%							
SiO_2	28.2	21.94	26.91	30.02	37.47	34.67	37.50	27.61	26.11	23.96	37.81	33.80	32.03	39.16
FeO_t	31.45	36.88	31.15	26.73	19.58	20.37	16.09	28.87	29.43	35.46	18.46	21.50	19.49	16.74
Al_2O_3	17.18	17.10	17.24	18.01	14.68	13.19	11.95	13.90	15.17	13.88	13.38	12.17	12.39	11.35
TiO_2	10.18	10.70	10.20	8.92	6.95	7.08	5.36	9.89	10.25	10.95	7.31	6.75	6.36	5.63
CaO	0.09	0.08	0.10	0.10	5.43	7.47	11.15	0.65	0.96	1.00	3.50	7.35	9.86	11.43
MgO	0.90	0.81	0.84	1.04	4.50	5.10	7.37	1.90	2.07	2.16	3.67	7.97	6.55	7.47
P_2O_5	0.39	0.31	0.37	0.45	1.36	1.23	1.48	0.86	1.04	0.90	0.86	1.56	1.29	1.27
Na_2O	0.05	0.07	0.07	0.17	0.53	0.41	0.57	0.18	0.19	0.23	0.29	0.48	0.63	0.92
K_2O	0.03	0.04	0.05	0.07	0.15	0.37	0.27	0.63	0.68	0.88	0.48	0.32	0.27	0.34
MnO	0.48	0.39	0.47	0.45	0.30	0.34	0.27	0.36	0.38	0.41	0.30	0.27	0.24	0.22
LOI	11.05	11.68	12.60	14.03	9.05	9.79	7.99	15.15	13.71	10.17	13.95	7.82	10.89	5.48
Total	100.00	100.00	100.00	100.00	100.00	100.00	100.00	100.00	100.00	100.00	100.00	100.00	100.00	100.00
							mg kg^{-1}							
Ba	2724.73	2916.77	2907.94	2293.72	1377.45	1426.84	1608.22	1422.68	1439.27	1786.25	1887.55	1069.01	850.11	852.91
Co	252.51	257.73	248.08	185.76	127.12	86.38	92.73	176.60	177.42	193.78	116.35	122.91	74.05	69.07
Cr	751.27	643.95	596.31	478.44	252.82	578.50	363.23	683.44	714.72	682.87	472.19	560.56	269.56	218.10
Cu	64.10	57.27	54.58	64.37	44.73	80.54	75.90	74.01	84.62	76.33	87.47	60.45	56.30	82.09
Li	9.24	10.07	15.20	22.07	14.35	12.55	10.94	22.76	26.46	23.95	9.69	10.85	< LQ	< LQ
Ni	226.73	232.70	232.73	204.51	115.04	119.72	127.93	187.52	223.57	184.52	115.02	145.57	108.55	80.91
Sr	482.29	615.96	625.91	567.67	1240.76	1054.46	1592.12	469.31	428.65	724.35	566.09	821.77	871.48	858.86
Th	40.12	39.46	37.80	30.50	33.40	37.97	39.50	26.52	28.34	34.50	32.02	30.88	29.60	30.21
V	313.97	353.05	299.32	247.72	248.97	334.69	302.20	465.91	485.33	425.56	275.81	305.18	247.86	255.17
Zn	211.01	206.70	203.02	202.32	145.55	151.26	128.11	178.16	182.52	215.66	172.75	151.72	134.15	144.44
Be	0.58	< LQ	0.87	1.27	1.08	1.26	1.00	1.21	1.23	1.56	1.13	0.76	0.62	0.99
Zr	439.82	463.95	444.32	373.15	314.24	347.24	279.70	447.85	460.68	511.87	308.19	367.80	325.71	296.98
S	1408.03	1519.63	1,260.70	300.59	220.20	262.83	110.88	355.97	564.24	86.81	65.44	213.50	70.96	< LQ
Sc	53.38	53.00	50.04	46.73	34.83	38.78	29.49	43.50	45.54	48.53	37.16	36.04	29.44	28.14
Ga	41.22	42.74	37.75	35.04	33.44	33.64	28.96	38.98	41.77	43.06	33.80	32.83	29.27	26.48
Y	17.53	15.12	12.93	13.86	42.62	51.25	48.56	54.55	54.42	63.60	41.28	43.68	38.52	38.90
Cd	1.73	1.67	1.82	3.23	1.86	1.27	0.88	1.78	2.30	2.71	0.75	0.94	0.63	0.49
In	0.21	0.23	0.19	0.18	0.15	0.15	0.12	0.20	0.21	0.22	0.16	0.15	0.14	0.13
Cs	0.07	0.12	0.15	0.31	1.04	1.59	0.75	1.41	1.48	1.92	0.62	0.51	0.28	0.18
Tl	< LQ	< LQ	< LQ	< LQ	< LQ	< LQ	< LQ	0.14	0.15	0.12	< LQ	< LQ	< LQ	< LQ
Pb	5.74	5.15	4.42	3.19	4.19	5.85	10.64	11.12	10.75	11.70	12.23	4.92	3.64	3.64
Bi	0.12	0.05	< LQ	< LQ	< LQ	< LQ	< LQ	0.06	0.08	0.06	0.043	0.05	0.04	< LQ
U	3.03	2.95	2.62	2.38	2.51	3.23	2.68	3.24	3.55	3.71	2.01	1.62	0.91	1.18
La	38.59	38.41	34.20	34.13	101.82	127.72	124.19	124.05	127.47	164.00	89.93	105.11	91.96	90.85
Ce	254.68	225.13	238.97	253.98	267.19	323.83	299.11	298.14	290.14	329.25	229.24	239.88	206.00	216.34
Pr	9.17	8.57	7.57	10.03	27.42	34.12	32.55	33.69	33.89	40.44	23.99	27.95	24.81	24.75
Nd	37.93	35.42	31.17	42.85	109.93	137.39	131.87	137.46	136.28	169.70	97.44	111.06	98.49	98.66
Sm	9.15	9.14	7.99	11.02	20.58	25.49	24.14	26.09	25.98	31.68	18.72	20.97	18.63	18.58
Eu	3.21	3.22	2.82	3.62	6.34	7.63	7.28	7.88	7.90	9.24	5.85	6.42	5.64	5.61
Gd	8.24	7.61	6.81	8.53	18.01	21.80	20.60	22.33	22.27	25.87	16.37	18.08	16.00	15.95
Tb	0.99	0.93	0.83	1.05	2.00	2.44	2.25	2.52	2.56	2.90	1.87	2.05	1.82	1.81
Dy	5.55	5.16	4.61	5.74	10.10	12.44	11.26	13.12	13.23	14.96	9.67	10.42	9.24	9.24
Ho	0.93	0.86	0.76	0.92	1.67	2.07	1.87	2.17	2.20	2.50	1.64	1.72	1.53	1.52
Er	2.34	2.17	1.93	2.32	4.03	5.14	4.66	5.28	5.38	6.10	4.04	4.20	3.74	3.68
Tm	0.30	0.27	0.24	0.29	0.46	0.58	0.53	0.61	0.63	0.71	0.48	0.48	0.42	0.42
Yb	1.75	1.61	1.46	1.84	2.56	3.36	3.04	3.51	3.55	3.99	2.68	2.67	2.40	2.40
Lu	0.23	0.21	0.18	0.23	0.35	0.46	0.41	0.47	0.47	0.54	0.36	0.36	0.32	0.32

LQ: quantification limits; LOI: loss on ignition; A, Bi, C1, C2 and C: soil horizons; Py: pyroclasts.

horizon and a more pronounced increase in the Bi horizon followed by a decrease in the A horizon. Among these elements, S is the one with significant gain of 511.24% in the Bi horizon while Th, V and Ga have relative loss of 14.20, 9.92 and 11.95%, respectively. Sr and Be behavior is the reverse of Ba, Co, Cr e Ni, that is, occur a decrease towards the top of the profile with higher loss of Sr and Be in the A horizon. The Y presents similar loss in all horizons with values around 70%.

For the REEs occur a decrease of all elements toward the top of the profile, except Sc that presents increase. Among them, the Dy, Er, Yb, La and Nd show a peak increase in the Bi horizon and, in particular, of Ce in the C1 horizon. The geochemical balance shows less loss in the Bi horizon except the Ce which has the lowest value in the C1 horizon. The greatest losses are of LREEs with values around 60–80%, except the Ce with value between 19–35%. The HREEs show moderate losses of around 40–60%.

Profile 3

Among the major and minor elements, the absolute contents of Fe, Ti and K increase in the C2 and C1 horizon and decrease in the A horizon. The geochemical balance shows higher gain of 39.70 and 33.33% for Fe and K, respectively, in the C2 horizon. The elements Si, Al, Ca, Mg, P, Na and Mn decrease towards the top of the profile with more pronounced loss for Ca around 79–90%.

The absolute contents of Ba, Cu, Sr, Th, Zn, Sc, Ga decrease towards the top of the profile and those of S, Cd and U increase. Co, Cr, Li, Ni, V, Be, Zr, Y and Cs increase in C2 and C1 horizon and decrease in the A horizon. The chemical elements In and Bi present constant behavior with a small decrease in the A horizon. The geochemical balance shows loss of Ba, Sr, Th, Zn, Sc, Cu, Ga, Be and Y in relation to pyroclast with greater loss in the A horizon around 30–60%, as opposed to Li, Cd and Cs that show gain in all horizons. Co, Cr, Ni, V and Zr have

Table 3. Concentration results, in mg.kg^{-1}, and their normalization to chondrite (McDonough and Sun 1995), for rare earth elements in profiles 1,2, 3 and 4.

Prof.	Hor.	La	Ce	Pr	Nd	Sm	Eu	Gd	Tb	Dy	Ho	Er	Tm	Yb	Lu	ΣLREE	ΣHREE	LREE/ HREE	La/Lu	Ce/ Ce*	Eu/ Eu*
1	A	128.63	303.19	76.42	65.40	43.57	43.38	27.47	20.20	17.90	12.74	11.14	9.09	8.75	7.42	617.21	114.72	5.38	17.34	2.82	1.21
	Bi	128.03	268.01	71.42	61.07	43.52	43.51	25.37	18.98	16.65	11.78	10.33	8.18	8.05	6.77	572.05	106.11	5.39	18.90	2.54	1.23
	C1	114.00	284.49	63.08	53.74	38.05	38.11	22.70	16.94	14.87	10.41	9.19	7.27	7.30	5.81	553.36	94.49	5.86	19.63	3.03	1.23
	C2	113.77	302.36	83.58	73.88	52.48	48.92	28.43	21.43	18.52	12.60	11.05	8.79	9.20	7.42	626.06	117.44	5.33	15.33	3.01	1.16
	Py	339.40	318.08	228.50	189.53	98.00	85.68	60.03	40.82	32.58	22.88	19.19	13.94	12.80	11.29	1173.52	213.53	5.50	30.06	1.10	1.09
2	C	425.73	385.51	284.33	236.88	121.38	103.11	72.67	49.80	40.13	28.36	24.48	17.58	16.80	14.84	1453.84	264.64	5.49	28.69	1.06	1.06
	Py	413.97	356.08	271.25	227.36	114.95	98.38	68.67	45.92	36.32	25.62	22.19	16.06	15.20	13.23	1383.61	243.20	5.69	31.30	1.01	1.07
3	A	413.50	354.93	280.75	237.00	124.24	106.49	74.43	51.43	42.32	29.73	25.14	18.48	17.55	15.16	1410.42	274.25	5.14	27.27	1.00	1.07
	C1	424.90	345.40	282.42	234.97	123.71	106.76	74.23	52.24	42.68	30.14	25.62	19.09	17.75	15.16	1411.40	276.91	5.10	28.03	0.96	1.07
	C2	546.67	391.96	337.00	292.59	150.86	124.86	86.23	59.18	48.26	34.25	29.05	21.52	19.95	17.42	1719.07	315.85	5.44	31.38	0.85	1.04
	Py	299.77	272.90	199.92	168.00	89.14	79.05	54.57	38.16	9.67	22.47	4.04	14.55	13.40	11.61	1029.73	168.46	6.11	25.81	1.07	1.10
4	A	350.37	285.57	232.92	191.48	99.86	86.76	60.27	41.84	33.61	23.56	20.00	14.55	13.35	11.61	1160.19	218.79	5.30	30.17	0.96	1.08
	C1	306.53	245.24	206.75	169.81	88.71	76.22	53.33	37.14	29.81	20.96	17.81	12.73	12.00	10.32	1017.05	194.10	5.24	29.70	0.94	1.07
	C2	302.83	257.55	206.25	170.10	88.48	75.81	53.17	36.94	29.81	20.82	17.52	12.73	12.00	10.32	1025.21	193.31	5.30	29.34	1.00	1.06

Prof.: profile; Hor.: pedological horizons; Py: pyroclast; (La/Lu)ch: (La/Lach)/(Lu/Luch); Ce/Ce*: (3Ce/Cech)/(2La/Lach + Nd/Ndch); Eu/Eu*: (3Eu/Euch)/(2Sm/Smch + Tb/Tbch); ch: concentration in chondrite; HREE: high rare earth elements; LREE: low rare earth elements.

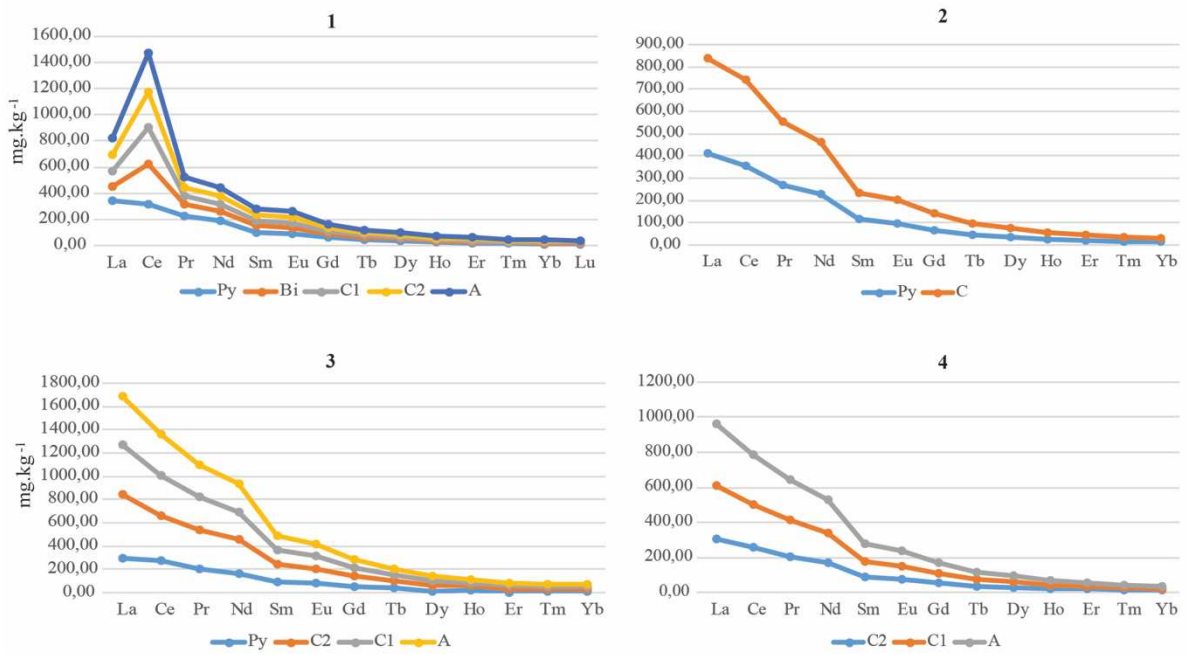

Figure 2. Typical chondrite-normalized rare earth elements plots of soils and pyroclasts of profiles 1, 2, 3 and 4.

gains in C2 and C1 horizon and loss in the A horizon. S is the element with the highest gain (559.73%) between the trace elements. Be and Y behave differently from other trace elements.

For the REEs occur an increase in absolute values from rock to C2 horizon followed by a decrease towards the top of the profile. The geochemical balance shows gain of all elements in the C2 and C1 horizons, except for Ce and Lu that present small loss of 3.11 and 0.11%, respectively, and loss in the A horizon in relation to the pyroclast. In addition, the LREEs show higher gains than the HREEs, between 14–33% and 9–12%, respectively.

DISCUSSION

According to weather studies of geochemical evolution of soil profiles, in all studied profiles the amount of silica

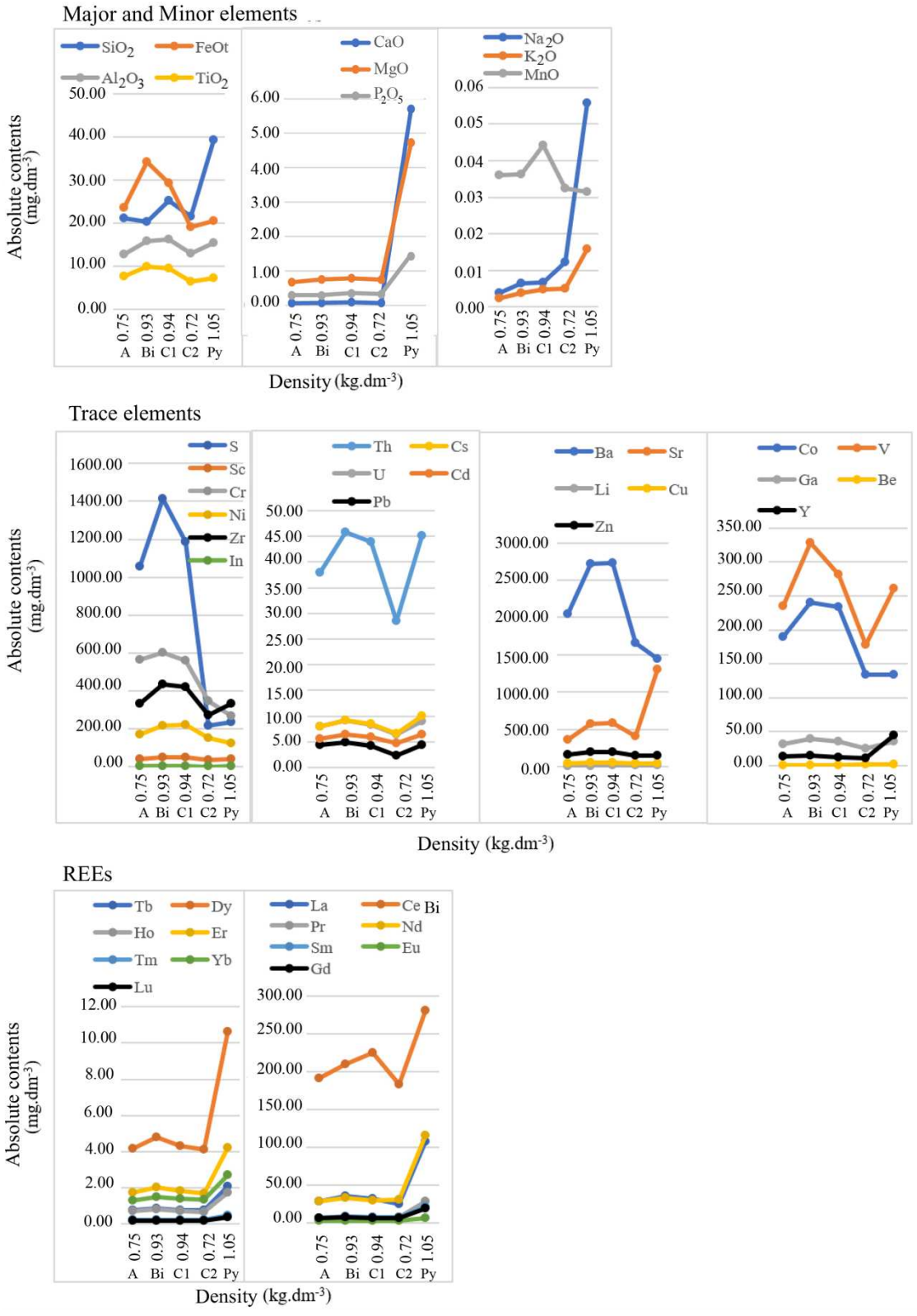

REEs: rare earth elements.

Figure 3. Comparison between densities and absolute contents from profile 1.

decreases considerably with the advance of weathering, while aluminum, iron and titanium tend to accumulate due to their low mobility. Calcium, sodium, potassium and magnesium are the most intensely leached. In the profile 4, potassium and magnesium values are slightly high in the A horizon due to the position of this profile at a lower altitude. The influence of saline sprays and the deposition of chemical elements from the higher regions increase the amounts of chemical elements in the profiles located at lower altitude, corroborating with Clemente *et al.* (2012).

Profiles located at higher altitudes, such as profile 1 (460 m), are most depleted in the most mobile elements such as Na, Ca, Mg and K. Clemente *et al.* (2012) assigned the low values of CaO to acid pH, to greater degree of weathering in

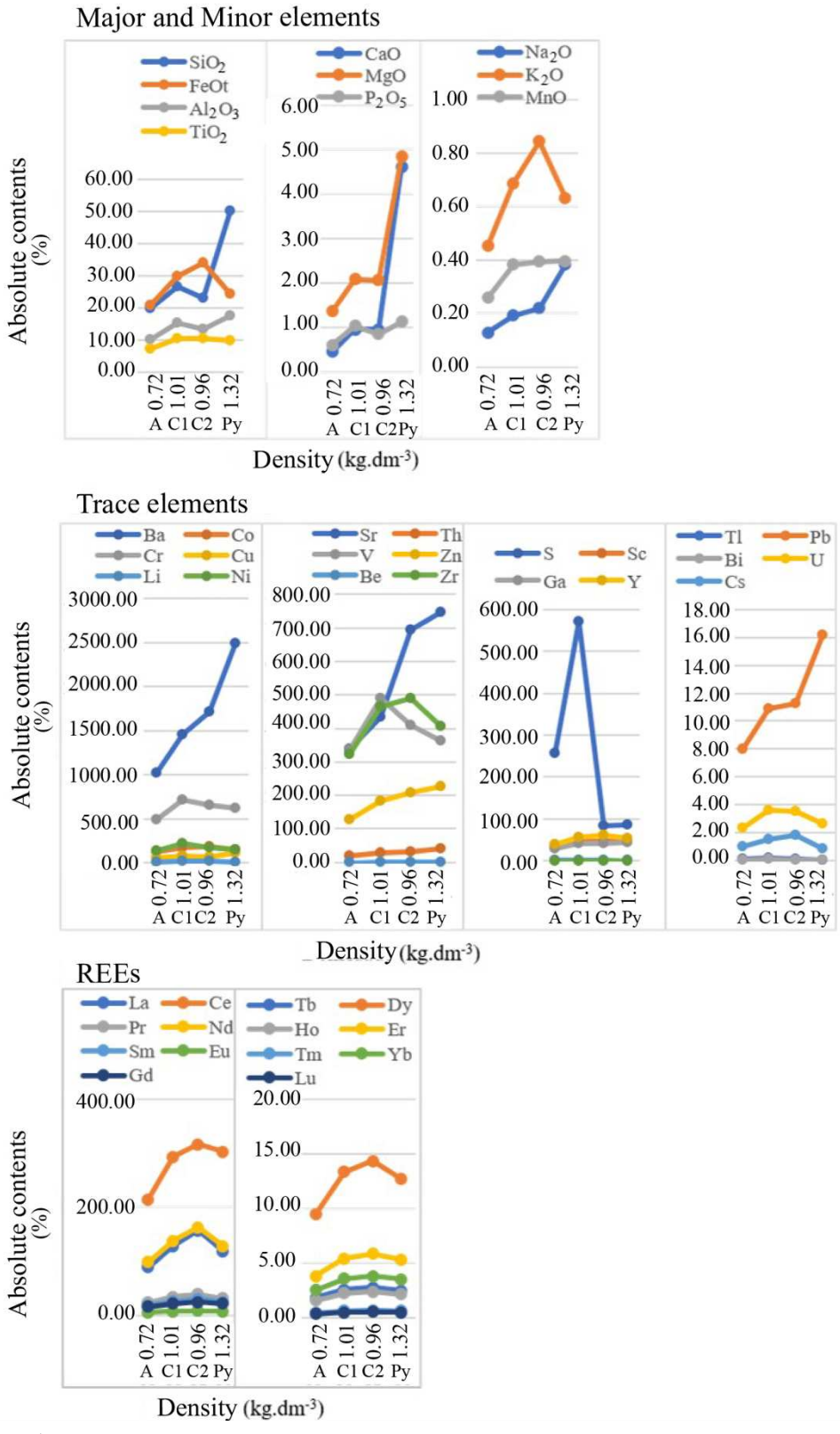

REEs: rare earth elements.

Figure 4. Comparison between densities and absolute levels from profile 3.

Table 4. Absolute values of the major, minor and trace elements and rare earth elements from profiles 1 and 3.

Profiles	**1**					**3**			
Horizons and rocks	**A**	**Bi**	**C1**	**C2**	**Py**	**A**	**C1**	**C2**	**Py**
				kg dm^{-3}					
Bulk	0.75	0.93	0.94	0.72	1.05	0.72	1.01	0.96	1.32
				%					
SiO_2	21.15	20.40	25.30	21.61	39.34	19.88	26.37	23.00	49.91
FeO_t	23.59	34.30	29.28	19.25	20.56	20.79	29.72	34.04	24.37
Al_2O_3	12.89	15.90	16.21	12.97	15.41	10.01	15.32	13.32	17.66
TiO_2	7.64	9.95	9.59	6.42	7.30	7.12	10.35	10.51	9.65
CaO	0.07	0.07	0.09	0.07	5.70	0.47	0.97	0.96	4.62
MgO	0.68	0.75	0.79	0.75	4.73	1.37	2.09	2.07	4.84
P_2O_5	0.29	0.29	0.35	0.32	1.43	0.62	1.05	0.86	1.14
Na_2O	0.04	0.07	0.07	0.12	0.56	0.13	0.19	0.22	0.38
K_2O	0.02	0.04	0.05	0.05	0.16	0.45	0.69	0.84	0.63
MnO	0.36	0.36	0.44	0.32	0.32	0.26	0.38	0.39	0.40
				mg dm^{-3}					
Ba	2,043.55	2,712.60	2,733.46	1,651.48	1,446.32	1,024.33	1,453.66	1,714.80	2,491.57
Co	189.38	239.69	233.20	133.75	133.48	127.15	179.19	186.03	153.58
Cr	563.45	598.87	560.53	344.48	265.46	492.08	721.87	655.56	623.29
Cu	48.08	53.26	51.31	46.35	46.97	53.29	85.47	73.28	115.46
Li	6.93	9.37	14.29	15.89	15.07	16.39	26.72	22.99	12.79
Ni	170.05	216.41	218.77	147.25	120.79	135.01	225.81	177.14	151.83
Sr	361.72	572.84	588.36	408.72	1302.80	337.90	432.94	695.38	747.24
Th	30.09	36.70	35.53	21.96	35.07	19.09	28.62	33.12	42.27
V	235.48	328.34	281.36	178.36	261.42	335.46	490.18	408.54	364.07
Zn	158.26	192.23	190.84	145.67	152.83	128.28	184.35	207.03	228.03
Be	0.44	-	0.82	0.91	1.13	0.87	1.24	1.50	1.49
Zr	329.87	431.47	417.66	268.67	329.95	322.45	465.29	491.40	406.81
S	1,056.02	1,413.26	1,185.06	216.42	231.21	256.30	569.88	83.34	86.38
Sc	40.04	49.29	47.04	33.65	36.57	31.32	46.00	46.59	49.05
Ga	30.92	39.75	35.49	25.23	35.11	28.07	42.19	41.34	44.62
Y	13.15	14.06	12.15	9.98	44.75	39.28	54.96	61.06	54.49
Cd	1.30	1.55	1.71	2.33	1.95	1.28	2.32	2.60	0.99
In	0.16	0.21	0.18	0.13	0.16	0.14	0.21	0.21	0.21
Tl	-	-	-	-	-	0.10	0.15	0.12	-
Pb	4.31	4.79	4.15	2.30	4.40	8.01	10.86	11.23	16.14
Bi	0.09	0.05	-	-	-	0.04	0.08	0.06	0.06
U	2.27	2.74	2.46	1.71	2.64	2.33	3.59	3.56	2.65
Cs	0.05	0.11	0.14	0.22	1.09	1.02	1.49	1.84	0.82
La	28.94	35.72	32.15	24.57	106.91	89.32	128.74	157.44	118.71
Ce	191.01	209.37	224.63	182.87	280.55	214.66	293.04	316.08	302.60
Pr	6.88	7.97	7.12	7.22	28.79	24.26	34.23	38.82	31.67
Nd	28.45	32.94	29.30	30.85	115.43	98.97	137.64	162.91	128.62
Sm	6.86	8.50	7.51	7.93	21.61	18.78	26.24	30.41	24.71
Eu	2.41	2.99	2.65	2.61	6.66	5.67	7.98	8.87	7.72
Gd	6.18	7.08	6.40	6.14	18.91	16.08	22.49	24.84	21.61
Tb	0.74	0.86	0.78	0.76	2.10	1.81	2.59	2.78	2.47
Dy	4.16	4.80	4.33	4.13	10.61	9.45	13.36	14.36	12.76
Ho	0.70	0.80	0.71	0.66	1.75	1.56	2.22	2.40	2.16
Er	1.76	2.02	1.81	1.67	4.23	3.80	5.43	5.86	5.33
Tm	0.23	0.25	0.23	0.21	0.48	0.44	0.64	0.68	0.63
Yb	1.31	1.50	1.37	1.32	2.69	2.53	3.59	3.83	3.54
Lu	0.17	0.20	0.17	0.17	0.37	0.34	0.47	0.52	0.48

Hor.: pedological horizons; Py: pyroclast.

Table 5. Mass balance of profiles 1 and 3.

Profiles	**1**				**3**		
Hor. and rocks	**A-py**	**Bi-py**	**C1-py**	**C2-py**	**A-py**	**C1-py**	**C2-py**
				%			
SiO_2	-46.24	-48.14	-35.71	-45.06	-60.17	-47.16	-53.91
FeO_t	14.73	66.83	42.42	-6.39	-14.70	21.98	39.70
Al_2O_3	-16.41	3.17	5.14	-15.87	-43.33	-13.25	-24.55
TiO_2	4.62	36.36	31.39	-11.99	-26.20	7.29	8.94
CaO	-98.82	-98.70	-98.35	-98.74	-89.87	-79.01	-79.22
MgO	-85.71	-84.06	-83.29	-84.15	-71.76	-56.84	-57.20
P_2O_5	-79.52	-79.81	-75.64	-77.31	-45.45	-7.47	-23.89
Na_2O	-93.26	-88.30	-88.18	-78.01	-66.14	-49.87	-42.32
K_2O	-85.71	-76.38	-70.16	-68.00	-28.41	8.40	33.33
MnO	14.29	15.14	40.25	2.86	-34.55	-3.08	-0.61
Ba	41.29	87.55	88.99	14.18	-58.89	-41.66	-31.18
Co	41.89	79.57	74.71	0.20	-17.21	16.68	21.13
Cr	112.25	125.60	111.15	29.77	-21.05	15.82	5.18
Cu	2.36	13.40	9.24	-1.32	-53.85	-25.98	-36.54
Li	-54.01	-37.85	-5.17	5.46	28.12	108.94	79.75
Ni	40.78	79.16	81.11	21.90	-11.07	48.73	16.67
Sr	-72.24	-56.03	-54.84	-68.63	-54.78	-42.06	-6.94
Th	-14.20	4.64	1.32	-37.38	-54.82	-32.28	-21.64
V	-9.92	25.60	7.63	-31.77	-7.86	34.64	12.21
Zn	3.55	25.78	24.87	-4.68	-43.75	-19.16	-9.21
Be	-61.64	-	-27.88	-19.37	-41.59	-16.71	0.40
Zr	-0.03	30.77	26.58	-18.57	-20.74	14.37	20.79
S	356.74	511.24	412.55	-6.39	196.71	559.73	-3.52
Sc	9.47	34.78	28.62	-8.00	-36.15	-6.23	-5.02
Ga	-11.95	13.20	1.06	-28.15	-37.10	-5.44	-7.35
Y	-70.62	-68.58	-72.84	-77.70	-27.92	0.87	12.05
Cd	-33.56	-20.48	-12.40	19.08	29.45	134.65	162.79
In	0.00	35.81	13.40	-17.71	-31.82	0.43	0.00
Cs	-95.19	-89.78	-87.09	-79.56	24.05	82.65	125.22
Pb	-2.15	8.86	-5.56	-47.79	-50.41	-32.74	-30.42
Bi	-	-	-	-	-23.89	42.35	1.48
U	-13.77	4.10	-6.55	-34.98	-12.08	35.14	34.24
La	-72.93	-66.59	-69.93	-77.01	-24.76	8.46	32.63
Ce	-31.92	-25.37	-19.93	-34.82	-29.06	-3.16	4.46
Pr	-76.11	-72.32	-75.28	-74.92	-23.40	8.09	22.60
Nd	-75.35	-71.46	-74.62	-73.27	-23.05	7.01	26.66
Sm	-68.24	-60.66	-65.24	-63.28	-23.98	6.19	23.08
Eu	-63.84	-55.02	-60.18	-60.85	-26.53	3.33	14.87
Gd	-67.32	-62.57	-66.15	-67.52	-25.60	4.09	14.93
Tb	-64.64	-58.81	-62.85	-64.00	-26.49	4.75	12.79
Dy	-60.75	-54.75	-59.14	-61.03	-25.99	4.68	12.51
Ho	-60.22	-54.39	-59.26	-62.22	-27.83	2.64	10.86
Er	-58.53	-52.31	-57.13	-60.52	-28.71	1.89	9.81
Tm	-53.42	-48.01	-53.29	-56.77	-30.68	0.43	7.58
Yb	-51.17	-44.30	-48.94	-50.71	-28.56	1.35	8.28
Lu	-53.06	-46.86	-53.96	-54.94	-28.79	-0.11	9.09

Hor.: pedological horizons; Py: pyroclast.

region more elevated of Trindade Island and to small possibility of saline inputs. According to Mateus *et al.* (2020a), acid pH data around 5 were found for C1, Bi and A horizons from the profile 1, which may justify the low CaO values in this profile.

In all profiles, the trace elements Ba, Co, Cr, Ni, Sr, V, Zn, Zr, S and Ce are the most abundant and, in general, their quantities increase towards the top of the profile. Similar behavior was found in Fernando de Noronha Island for Co, Cr and Ni in soils developed from rocks of mafic composition (Oliveira *et al.* 2011b). High values of Ba may be related to Ti-biotite, since Marques *et al.* (1999) and Greenwood (1998) reported its presence in heavily zoned Ti-biotite in ultramafic rocks (melanephelinites) from Trindade Island. The presence of ferromagnesian minerals such as olivine, pyroxene and amphibole explain the high content of Ni, Cr, Co, Zn and V. According to Hawes and Webb (1962), Ni, Cr, Co, Cu, Zn and V have similar chemical characteristics and occur in ferromagnesian minerals. Cr contents is high for all soils due to the deep mantelic origin of the pyroclasts and tend to concentrated in the olivine nuclei (Mateus *et al.* 2020b). This fact explains the high exchangeable levels of Cr in soils from the Morro Vermelho Formation (Clemente *et al.* 2012). The Cu content from profiles 3 and 4 present similar behavior to the soils of Clemente *et al.* (2012): higher content in near-sea soils, at lower altitude and in younger soils. Another similarity to the Clemente *et al.* (2012) study is the most pronounced Zn content in horizons with greater amount of organic matter such as the A horizon of profile 3 and 4, with values of 18.03 e 9.39 $g.kg^{-1}$ in total organic carbon respectively (Mateus *et al.* 2020a). According to Abreu *et al.* (2001), high levels of organic matter can complex Cu and Zn retaining these elements in the soil. Therefore, the higher levels of Zn and Cu in the A horizon from profiles 3 and 4 would be a consequence of the greater amounts of complexes of humic acid linked to these elements. In addition, all horizons from the profiles 3 and 4 still contain several relict fragments of the parental rock (Mateus *et al.* 2020a), which could contribute to the more pronounced presence of Zn and Cu.

For profiles 1 and 3, the gain of Fe, Ti, Al and Mn are relative, as these elements increase due to the detriment of others such as Si, Na, K, Ca, Mg and P. In relation to trace elements, profile 1 shows moderate mobility of Sr, V, Co, Y, Zr, Pb, Cd, U, Cs, Th, Ga characterized by the loss of these elements from the altered rock to the C2 horizon and a relative enrichment, especially in Bi horizon. Ba, Cr and Ni show enrichment towards to the top of the profile. Li, Zn, Be, Sc do not vary much and show very close values in the rock and in the soil.

Profile 3 has the inverse behavior of profile 1, with high mobility for Ba, Sr, Zn, Pb represented by their marked loss to the top of the profile and a relative enrichment of Cr, Ni, Co, Zr, V, S, Y, Ga, U, Cs from rock to soil, with slight loss in the A horizon. According to Hawes and Webb (1962) Ba and Sr are elements of high mobility, corroborating the geochemical behavior found in the soils of this study. Li, Be and Bi are constant in the profile 1 e 3.

All profiles showed high concentration of LREE. Featured, the profiles 1 and 2 showed positive Ce anomalies, with higher values in 1. In soils on basaltics pyroclasts from São Miguel island (Azores archipelago) occur similar behavior (Freitas and Pacheco 2010) as in topsoils on phonolitic pyroclasts in Brava Island (Cape Verde archipelago); Marques *et al.* (2018) related the relative Ce enrichment to stronger oxidizing conditions leading to $Ce^{3+} \rightarrow Ce^{4+}$ with preferred retention of this element on the clay-size fraction. This same explanation could be applied to soil from profile 1 since it is the profile that is most weathered (Mateus *et al.* 2018).

The REEs in profile 1 are lost by leaching. The position of this profile in higher regions contributes to the loss of these elements. The opposite occurs in the profile 3 positioned in lower regions, concentrating these elements at the base of the profile (C2 and C1 horizon), highlighting the LREEs that show larger gain than the HREEs. In the Fernando de Noronha Island, the HREEs accumulate in soils on mafic rocks (nepheline basalts) at low altitude (Oliveira *et al.* 2011a). One explanation for this difference would be that the profile studied by Oliveira *et al.* (2011a) is located on older rocks Morro Quixaba Formation (6.2 Ma, Perlingeiro *et al.* 2013) that of the Morro Vermelho Formation (0.17 Ma, Cordani 1970), and consequently the soils formed on these rocks are more weathered and more leached, concentrating more HREE than LREE.

CONCLUSIONS

In all profiles, Al and Fe accumulate towards to the top due to their low mobility, and, Ca, Na, K and Mg are the most intensely leached. Similarly, Ti, Mn, Co, Cr, Ni, V, Zr, S show relative enrichment due to the leaching of the most mobile elements during the soil formation process.

Lower altitude profiles tend to have higher K and Mg values in A horizon due to the influence of saline sprays.

Zn and Cu are concentrated in A horizon of low altitude profiles that have higher organic matter content and relict fragments of parental rock.

Leaching of the REEs from higher to the lower slope led to the enrichment of these elements, especially the light REEs, in the low lying (258 m) soil. The Ce positive anomalies in high altitude profile (460 m) is because it is more weathered.

ACKNOWLEGEMENTS

We would like to thank to the Brazilian Navy for their logistical support and to the CNPq (306424/2016-9; 442730/2015-2), CAPES (Finance code 001) and FAPEMIG (PPM-00326-18) for their financial contribution. We would also like to express our gratitude to the Laboratory of Environmental Geochemistry (LGqA) of DEGEO/UFOP for the geochemical analyses. Lastly, we would like to show our appreciation to the Laboratory of X-Ray Diffraction of DEGEO/UFOP and of IC2MP, Université de Poitiers for the mineralogical analyses. Authors also acknowledged financial support from the European Union (ERDF) and Region Nouvelle Aquitaine.

ARTICLE INFORMATION
Manuscript ID: 20200073. Received on: 12/30/2019. Approved on: 08/28/2020.
A.C.C.M. wrote the first draft of the manuscript and prepared Figures 1, 2, 3, 4 and Tables 1, 2, 3, 4 and 5. A.C.C.M. was responsible for the geochemical analysis acquisition. A.F.D.C.V., F.S.O., S.P. and C.E.G.R.S. provided advisorship regarding geochemistry, geology, pedology and improved the manuscript through corrections and suggestions. A.F.D.C.V. and C.E.G.R.S. revised the English. A.F.D.C.V., F.S.O., S.P. and C.E.G.R.S. were responsible for the acquisition of research funding.
Competing interests: The authors declare no competing interests.

REFERENCES

Abreu C.A., Ferreira M.E, Borkert C.M. 2001 Disponibilidade e avaliação de elementos catiônicos: zinco e cobre. *In*: Ferreira M.E., Cruz M.C.P., Raij B. van, Abreu C.A. (eds.). *Micronutrientes e elementos tóxicos na agricultura*. Jaboticabal: CNPq/FAPESP/POTAFOS, p. 12-150.

Carvalho I.G. 1995. *Fundamentos da geoquímica dos processos exógenos*. Salvador: Bureau Gráfica e Editora, 213 p.

Clemente E.P., Schaefer C.E.R., Oliveira F.S., Marciano L.C., Clemente A.D. 2012. Geoquímica dos solos da Ilha da Trindade, Atlântico Sul, Brasil. *Geociências*, **31**(1):57-67.

Cordani U.G. 1970. Idade do vulcanismo do Oceano Atlântico Sul. *Boletim IAG USP*, **1**:9-75.

Cotta A.J.B., Enzweiler J., Nardy A.J.R. 2008. Certificado de Análise do Material de Referência BRP-1 (Basalto Ribeirão Preto). *Geochimica Brasiliensis*, **22**(2):113-118. http://dx.doi.org/10.21715/gb.v22i2.282

Cramer J.J., Nesbitt H.W. 1983. Mass-balance relations and trace-element mobility during continental weathering of various igneous rocks. *Sciences Géologiques*, **73**:63-73.

Freitas M.C., Pacheco A.M.G. 2010. Soils of Azores islands: elemental characterization with an emphasis on rare-earth elements. *Journal of Radioanalytical and Nuclear Chemistry*, **283**:117-122. https://doi.org/10.1007/s10967-009-0130-7

Fund W. 2014. *Trinidade-Martin Vaz Islands tropical forests*. Available from: <http://editors.eol.org/eoearth/wiki/Trinidade-Martin_Vaz_Islands_tropical_forests>. Accessed on: July 20, 2020.

Gardner L.R. 1980. Mobilization of Al and Ti during weathering-isovolumetric geochemical evidence. *Chemical Geology*, **30**(1-2):151-165. https://doi.org/10.1016/0009-2541(80)90122-9

Greenwood J.C. 1998. Barian–titanian micas from Ilha da Trindade, South Atlantic. *Mineralogical Magazine*, **62**(5):687-695. https://doi.org/10.1180/002646198547918

Hawes H.E., Webb J.S. 1962. *Geochemistry in Mineral Exploration*. New York: Elsevier, 377 p.

Manga V.E., Agyingi C.M., Suh C.E. 2016. Trace element behaviour in soils developed along the slopes of Mt. Cameroon, West Africa. *Geochemical Journal*, **50**(3):267-280. https://doi.org/10.2343/geochemj.2.0413

Marques R., Prudêncio M.I., Waerenborgh J.C., Rocha F., Dias M.I., Ruiz F., Ferreira da Silva E., Abad M., Muñoz A.M. 2014. Origin of reddening in a paleosol buried by lava flows in Fogo island (Cape Verde). *Journal of African Earth Sciences*, **96**:60-70. https://doi.org/10.1016/j.jafrearsci.2014.03.019

Marques L.S., Ulbrich M.N.C., Ruberti E., Tassinari C.G. 1999. Petrology, geochemistry and Sr-Nd isotopes of Trindade and Martin Vaz volcanic rocks (Southern Atlantic Ocean). *Journal of Volcanology and Geothermal Research*, **93**(3-4):191-216. https://doi.org/10.1016/S0377-0273(99)00111-0

Marques R., Vieira B.J., Prudêncio M.I., Waerenborgh J.C., Dias M.I., Rocha F. 2018. Chemistry of volcanic soils used for agriculture in Brava Island (Cape Verde) envisaging a sustainable management. *Journal of African Earth Sciences*, **147**:28-42. https://doi.org/10.1016/j.jafrearsci.2018.06.014

Mateus A.C.C., Varajão A.F.D.C., Oliveira F.S., Petit S., Schaefer C.E.R. 2020a. Non-allophanic andosols of trindade island, south atlantic, Brazil: A new soil orden in Brazil. *Revista Brasileira de Ciências dos Solos*, **44**:e0200007. http://dx.doi.org/10.36783/18069657rbcs20200007

Mateus A.C.C., Varajão A.F.D.C., Oliveira F.S., Schaefer C.E. 2018. Alteration of olivine in volcanic rocks from Trindade Island, South Atlantic. *Applied Clay Science*, **160**:40-48. https://doi.org/10.1016/j.clay.2018.01.033

Mateus A.C.C., Varajão A.F.D.C., Petit S., Oliveira F.S., Schaefer C.E.G.R. 2020b. Mineralogical and geochemical signatures of Quaternary pyroclasts alterations at the volcanic Trindade Island, South Atlantic**.** *Journal of South American Earth Sciences*, **102**:102674. https://doi.org/10.1016/j.jsames.2020.102674

McDonough W.F., Sun S.S. 1995. The composition of the earth. *Chemical Geology*, **120**(3-4):223-253. https://doi.org/10.1016/0009-2541(94)00140-4

Millot G., Bonifas M. 1955. Transformations isovolumetriques dans les phenomenes de laterisation et de bauxitisation. *Bulletin Service Carte Géolique d'Alsace et Lorraine*, **8**:3-20.

Oliveira F.S., Shaefer C.E.G.R., Abrahão W.A.P., Clemente E.P., Simas F.N.B. 2014. Soil–geomorphology interactions and paleoclimatic implications of an ornithogenic soil toposequence on Rata Island, Fernando de Noronha Archipelago, South Atlantic. *Journal of South American Earth Sciences*, **52**:119-128. https://doi.org/10.1016/j.jsames.2014.02.007

Oliveira S.M.B., Pessenda L.C.R., Babinski M., Gioia S.M.C.L., Fávaro D.I.T. 2011a. Solos Desenvolvidos Sobre Diferentes Rochas Vulcânicas da Ilha de Fernando de Noronha: Padrão de Elementos Terras Raras e Composição Isotópica do Chumbo. *Revista do Instituto de Geociências*, **11**(3):97-105. https://doi.org/10.5327/Z1519-874X2011000300006

Oliveira S.M.B., Pessenda L.C.R., Gouveia S.E.M., Fávaro D.I.T. 2011b. Heavy metal concentrations in soils from a remote oceanic island, Fernando de Noronha, Brazil. *Anais da Academia Brasileira de Ciências*, **83**(4):1193-1206. http://dx.doi.org/10.1590/S0001-37652011005000042

Oliveira S.M.B., Pessenda L.C.R., Gouveia S.E.M., Fávaro D.I.T., Babinski M. 2009. Evidência Geoquímica de Solos Formados pela Interação de Guanos com Rochas Vulcânicas, Ilha Rata, Fernando de Noronha (PE). *Revista do Instituto de Geociências*, **9**(3):3-12. http://dx.doi.org/10.5327/z1519-874x2009000300001

Perlingeiro G., Vasconcelos P.M., Knesel K.M., Thiede D.S., Cordani U.G. 2013. 40Ar/39Ar geochronology of the Fernando de Noronha Archipelago and implications for the origin of alkaline volcanism in the NE Brazil. *Journal of Volcanology and Geothermal Research*, **249**:140-154.

Putnis A. 2009. Mineral Replacement Reactions. *Reviews in Mineralogy and Geochemistry*, **70**(1):87-124. https://doi.org/10.2138/rmg.2009.70.3

Roca N., Pazos M.S., Bech, J. 2008. The relationship between WRB soil units and heavy metals content in soils of Catamarca (Argentina). *Journal of Geochemical Exploration*, **96**(2-3):77-85. https://doi.org/10.1016/j.gexplo.2007.04.004

Teixeira P.C., Donagemma G.K., Fontana A., Teixeira W.G. 2017. *Manual de métodos de análise de solo*. Brasília: Embrapa, 573 p.

Vieira B.J., Soares P.M., Prudêncio M.I., Freitas M.C., Rodrigues A.F. 2004. Caracterização química (terras raras e outros elementos) de solos das ilhas de Santa Maria e Terceira (Açores, Portugal). *Geociências*, **16**(1-2):5-12.